

1 **Identification of targets for drug repurposing to treat COVID-19 using a Deep**
2 **Learning Neural Network**

3 *Author names*

4 Si-Han Wang^{a#}, Yu-Hsuan Tang^{a#}, Hao Hsu^{a#}, Chu-Nien Yu^a, Oscar Kuang-Sheng
5 Lee^{a,b,c,d}

6 *Affiliations*

7 a) Institute of Clinical Medicine, National Yang Ming Chiao Tung University, Taipei,
8 Taiwan.

9 b) Stem Cell Research Center, National Yang Ming Chiao Tung University, Taipei,
10 Taiwan.

11 c) Department of Medical Research, Taipei Veterans General Hospital, Taipei,
12 Taiwan.

13 d) Department of Orthopedics, China Medical University Hospital, Taichung,
14 Taiwan.

15 #The equal contributions footnote specifies contributed to the manuscript equally.

16 *Contact information of the corresponding author:*

17 Oscar Kuang-Sheng Lee, MD, PhD

18 ORCID: 0000-0001-5232-5374

19 Tel: +886-2-28757391

20 Fax: +886-2-28757435

21 E-mail address: oscarlee9203@gmail.com

22

23 **Abstract**

24 The COVID-19 pandemic has resulted in a global public health crisis requiring
25 immediate acute therapeutic solutions. To address this challenge, we developed a useful
26 tool deep learning model using the graph-embedding convolution network (GECN)
27 algorithm. Our approach identified COVID-19-related genes and potential druggable
28 targets, including tyrosine kinase ABL1/2, pro-inflammatory cytokine CSF2, and pro-
29 fibrotic cytokines IL-4 and IL-13. These target genes are implicated in critical processes
30 related to COVID-19 pathogenesis, including endosomal membrane fusion, cytokine
31 storm, and tissue fibrosis. Our analysis revealed that ABL kinase inhibitors, lenzilumab
32 (anti-CSF2), and dupilumab (anti-IL4R α) represent promising therapeutic solutions
33 that can effectively block virus-host membrane fusion or attenuate hyperinflammation
34 in COVID-19 patients. Compared to the traditional drug screening process, our GECN
35 algorithm enables rapid analysis of disease-related human protein interaction networks
36 and prediction of candidate drug targets from a large-scale knowledge graph in a cost-
37 effective and efficient manner. Overall, Overall, our results suggest that the model has
38 the potential to facilitate drug repurposing and aid in the fight against COVID-19.

39

40

41 Word count of the article is 3604.

42 **1. Introduction**

43 Coronavirus disease 2019 (COVID-19) emerged in December 2019 and has
44 rapidly spread worldwide, resulting in a global public health crisis. Severe acute
45 respiratory syndrome coronavirus 2 (SARS-CoV-2), which causes COVID-19, is a
46 single-stranded positive RNA virus with spikes on its envelope [1]. As of 5 April 2023,
47 the World Health Organization COVID-19 Dashboard has reported 762,201,169
48 confirmed cases and 6,889,743 deaths worldwide. Many patients develop pneumonia
49 within weeks of showing symptoms and increased inflammatory cytokines which can
50 lead to respiratory failure and death [2]. The traditional drug discovery method, with a
51 long discovery period (10–15 years) and low success rate (2.01%) [3], has failed to
52 meet the urgent need for a COVID-19 cure.

53 Numerous monoclonal antibodies are currently being developed as systemic
54 therapies for COVID-19; however, their large size, instability, and low density of
55 binding sites (two per 150 KDa antibody) make them unsuitable for intranasal delivery
56 [4]. To overcome this challenge, deep learning, a subset of artificial intelligence (AI)
57 algorithms, can accelerate drug development and repurposing to slow down the
58 progression of acute disease. Deep learning uses multiple interconnected layers to
59 recognize complex patterns in data, which is useful for finding correlations between
60 inputs and outputs for complex problems. Unlike the traditional protein structure
61 prediction problem, locally connected graph neural networks can accurately model the
62 structure-to-sequence mapping problem [5]. The Graph Convolutional Network (GCN)
63 is an approach to graph embedding that transforms graph information into spectral
64 domains for convolutional calculation. This is done using the Laplacian matrix,
65 Chebyshev polynomials, or other methods [6-10]. GCNs are powerful in processing
66 network data, and their representative tasks include node classification, link prediction,
67 and graph generation., as they can combine features with a hidden layer to aggregate
68 important information from different nodes. By combining features with a hidden layer,
69 GCNs can effectively aggregate important information from different nodes. This
70 ability to recognize complex patterns in data and find correlations between inputs and
71 outputs for complex problems makes GCNs an excellent choice for prediction models.
72 Additionally, GCNs' locally connected graph neural networks can accurately model the
73 structure-to-sequence mapping problem, providing greater accuracy compared to
74 traditional protein structure prediction methods. Moreover, recent studies have shown

75 that deep learning, including GCNs, outperforms classic machine learning methods in
76 assisting drug repurposing, allowing the screening of existing drugs as potential
77 treatments for SARS-CoV-2. The development of affordable approaches for the
78 effective treatment of COVID-19 is challenging without foreknowledge of the complex
79 networks connecting drugs, targets, SARS-CoV-2, and diseases. Current studies
80 suggest that using the in-silico method to identified some potential antiviral drugs such
81 as remdesivir [11, 12], mefuparib [13], and toremifene [14, 15], while drugs like
82 baricitinib [16], melatonin [17], and dexamethasone [18, 19] have been identified as
83 potential host-targeted therapies to attenuate cytokine storms in COVID-19 patients.
84 The results of clinical trials for these drugs are controversial [20]. However, most of
85 these studies focused on SARS-CoV-2 proteins with known functions, such as the spike
86 protein and 3C-like (3CL) protease, or a host protein with a known interaction with
87 viruses, such as ACE2 and TMPRSS2. The approach of focusing only on SARS-CoV-
88 2 proteins and host proteins with known interactions with viruses significantly limits
89 the potential targets for drug development because the role and functional annotations
90 of many other host proteins are mostly ignored. In this study, we propose a new AI-
91 assisted drug development method, the graph-embedding convolution network (GECN),
92 that utilizes the functional annotations of host proteins to identify potential druggable
93 targets for SARS-CoV-2 pathogenic mechanisms. By investigating tissue specificity,
94 physiological functions, and cell signaling pathways, our approach aims to expedite
95 drug discovery new insights into the druggable targets and pathogenic mechanisms of
96 COVID-19.
97

98 2. Materials and Methods

99 2.1 Data preprocessing

100 The protein interaction data were extracted from the STRING dataset (v 11.0) [21] with
101 *Homo sapiens* axotomy (ID 9606), and edges between pairs of all associated genes
102 were constructed, regardless of whether it was physically binding or not. The edges
103 were not weighted, and no edge attributes were added. GO terms, such as cell
104 components, biological processes, and molecular functions, were extracted and
105 clustered using the semantic similarity method [22, 23]. In our study, semantic
106 similarity was represented by the minimum number of steps across the graph required
107 to connect two terms, weighted by how specific or general the terms are, and was
108 calculated with the following formula (2):

$$109 \quad Sim(go_i, go_j) = \frac{2 \cdot \max_{go \in S(go_i, go_j)} \{IC(go)\}}{IC(go_i) + IC(go_j)} \quad (2)$$

110 where go_i and go_j are a pair of GO terms and $Sim(go_i, go_j)$ are their semantic
111 similarities. $S(go_i, go_j)$ is the subset of GO terms shared between go_i and go_j after
112 propagating up the GO DAG using the “is_a” and “part_of” relations. $IC(go_i)$ is the
113 information content (IC) of a GO term, which is defined as the frequency of go_i ,
114 relative to the total number of GO terms in the UniProt Gene Ontology Annotation
115 (GOA) database [24, 25], specifically calculated using the formula (3):

$$116 \quad IC(GO_i) = -\log \left(\frac{\{go:go_i \in GOA\}}{\{go:go \in GOA\}} \right) \quad (3)$$

117 Pathway IDs from Reactome were clustered by propagating along the Reactome [26,
118 27] graph and were mapped to the top super pathway. Finally, the “probability of loss
119 of function intolerance” extracted from ExAC (v 1.0) [28] was normalized.

120

121 2.2 Graph convolution network (GCN)

122 The GCN algorithm included a feature matrix and an adjacency matrix [9]. A feature
123 matrix was $N \times F^0$ dimension, with N being the number of nodes and F^0 being the feature
124 numbers in each node. An adjacency matrix represented the structure of the graph, and
125 the dimension was $N \times N$.

126 Each neural network layer can be written as a non-linear function (4)[29], as shown
127 below, where $H(0) = X$ and $H(l) = Z$ (or z for graph-level outputs), and l is the number
128 of layers.

$$129 \quad H^{(l+1)} = f(H^{(l)}, A)$$

130 Here, $W^{(l)}$ is a weight matrix for the l -th neural network layer. Additionally, $\hat{A} = A +$
131 I , where I is the identity matrix, \hat{D} is the diagonal node degree matrix of \hat{A} , and $\sigma(\cdot)$ is
132 a non-linear activation function, like ReLU.

133 Besides, we use multilayer GCN to combine neighboring node features with self-loops
134 by summing and taking weighted average of their feature vectors which employ a
135 multilayer GCN with the following layer-wise propagation rule:

136

$$f(H^{(l)}, A) = \sigma(\hat{D}^{-1/2} \hat{A} \hat{D}^{-1/2} H^{(l)} W^{(l)})$$

137

138 The Variational Graph Autoencoder (VGA) is a type of neural network used for
139 generating molecular graphs and consists of an encoder and a decoder. The encoder of
140 the VGA, which employs edge condition convolution, embeds the original graph into a
141 continuous vector space. The decoder generates a probabilistic fully connected graph
142 according to the predefined number of nodes and updates the parameters through
143 approximate graph matching to improve the reconstruction ability of the autoencoder.

144 We constructed the VGA model using three layers of Graph Convolutional Network
145 (GCN) encoder with hidden unit dimensions of 512, 256, and 256, respectively. We
146 used an inner product decoder to produce the output. The VGA is a type of Variational
147 Autoencoder (VAE) that projects input features into a multivariate latent distribution
148 and samples the values of latent features from this distribution. To make the sampling
149 process differentiable and enable reliable training of the model, the reparameterization
150 trick is used. The reparameterization trick involves sampling from a standard normal
151 distribution and then transforming the sampled values to produce the latent features.
152 The formula for the reparameterization trick is given as (1):

153

$$z = \mu + \varepsilon \times \sigma \quad (1)$$

154 where $\varepsilon \sim N(0,1)$ and z is the latent feature. By using the reparameterization trick, the
155 model can backpropagate gradients through the sampling process, allowing for end-to-
156 end training of the variational autoencoder.

157

158 A neighbor sampler with a batch size of 1,024 was applied, and the loss function
159 contained reconstruction loss and KL loss. Reconstruction loss is the cross-entropy loss
160 of positive edges (interactions) and negative edges (non-interactions), whereas KL loss
161 is the KL divergence between the output distribution of encoder $N(\mu, \sigma)$ and standard
162 normal distribution $N(0,1)$. The AdamW optimizer was used [30], and 100 training

163 epochs were trained without early termination. Finally, the model with the best AUC
164 value was saved.

165 To predict potential links and appropriate evaluation of the performance of our
166 model, fixed-threshold metrics and test set sampling were required. We sampled those
167 negative edges where the geodesic distances were equal to 2. The shortest paths
168 between these pairs of nodes were equal to two, and improvements in these pairs were
169 weighted more than at greater distances. To decrease the computational complexity of
170 spectral graph convolution, the Chebyshev polynomial was used to replace the eigen-
171 decomposition of a Laplacian matrix [31]. The Chebyshev polynomial utilized the
172 recurrence relation to approach the value of eigen-decomposition and increase the
173 efficiency of model training. The hyperparameter k in the Chebyshev convolution
174 represents a receptive field that can lead the algorithm to see more local values. In our
175 model, we set k to 2. Cluster-GCN is a type of GCN algorithm that is suitable for
176 training by exploiting the graph clustering structure [32]. In this study, a graph
177 clustering algorithm identified a block of nodes associated with a dense subgraph. It
178 then restricted the neighborhood search within this subgraph. This simple but effective
179 strategy led to significantly improved memory and computational efficiency while
180 achieving a test accuracy comparable to that of previous algorithms.

181

182 **2.3 K-fold cross-validation**

183 K fold cross-validation was used to verify the performance of the model. It split the
184 data into five groups and randomly selected one of them as the test set. This approach
185 estimated the performance of the model using the new data.

186

187 **2.4 Protein-protein docking using MOE software**

188 *In silico* protein-protein docking of ABL1 against TNF and ABL2 against BTK was
189 performed using the MOE software [33]. PDB files of ABL1 (PDB ID: 1AWO), TNF
190 (PDB ID: 1TNF), ABL2 (PDB ID: 5NP3), and BTK (PDB ID: 5XYZ) were
191 downloaded from the RCSB PDB and imported into the MOE software. The pre-bound
192 ligands were first removed from the PDB structures. Protein structures were then
193 prepared using the MOE “Protein Preparation” tool (to correct atom lost issues) and
194 MOE “Protonate 3D” tool (to add hydrogen atoms and to assign ionization states
195 throughout the system). Water molecules farther than 4.5 Å from proteins were deleted.
196 Active sites of TNF and BTK were found using the MOE “Site Finder” tool (Compute,

197 Site Finder), and ABL1 or ABL2 were docked to all these sites later. Prepared structures
198 were docked by MOE “Dock” tool (Compute, Dock, Protein-protein). Docking
199 structures with a minimum S score indicated that the highest binding affinity was
200 selected for further interaction analyses. Interaction bond type, bond length, and bond
201 energy were indicated by MOE “Protein Contacts” tool (Protein, Protein Contacts).
202

203 **3. Results**

204 **3.1 Experiment setting of the graph embedding convolution network algorithm**

205 The GECN algorithm consists of two deep learning methods: GE and GCN, as shown
206 in Fig. 1. The GE model uses a Variational Graph Autoencoder (VGA) to extract latent
207 features from raw data, which are then used as input node features for the second deep
208 learning model, DeepGCN, to perform GCN as a classifier. The VGA encoder maps
209 raw data into a latent distribution with means and standard deviations, and a
210 reparameterization trick is employed to make the VGA suitable for backpropagation.
211 This makes the process of stochastic sampling of latent features from the latent
212 distribution differentiable. The decoder of the VGA reconstructs the latent features into
213 the adjacency matrix. The unsupervisedly trained VGA utilizes the reconstruction error
214 and Kullback-Leibler divergence to encode latent features, which are then fed as node
215 feature inputs into the supervisedly trained DeepGCN for classification. In brief,
216 DeepGCN utilizes a combination of latent features as nodes, PPI network as graph
217 structure, and disease-related genes as labels for training. The model is then trained
218 with focal loss to minimize the difference between predicted and true labels and is
219 enhanced with residual and dense connections for improved performance in comparison
220 to traditional GCN with a deeper structure. It predicts potential protein targets that
221 interact with COVID-19.

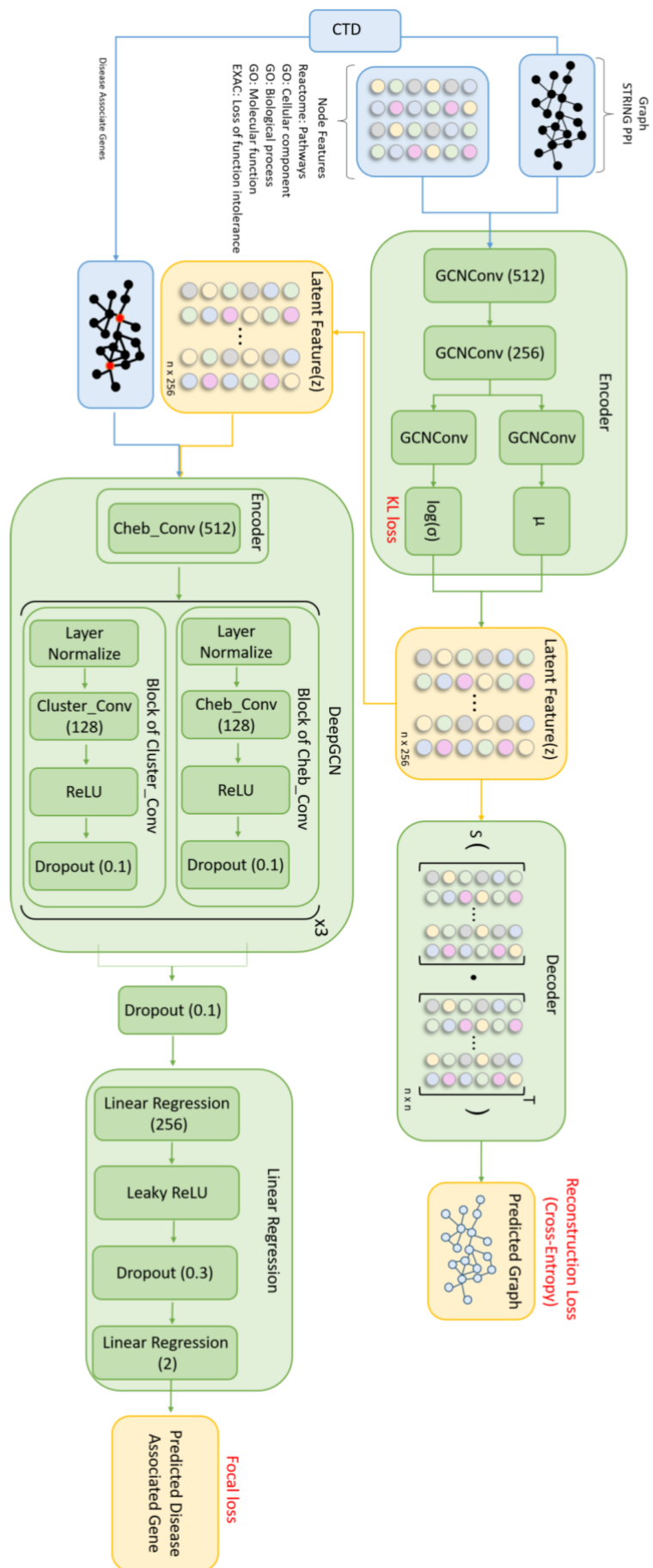
222

223 In this study, we conducted experiments on a biological network dataset consisting of
224 a total of 533,138 data points. These data points were divided into a training set and a
225 test set. The training set contained 479,825 positive edges, representing interactions
226 between pairs of genes. The test set included 53,313 positive edges and an equal number
227 of negative edges, representing the absence of interactions between pairs of genes. To
228 select the negative edges, we chose unconnected node pairs that had a geodesic distance
229 of two. This sampling strategy was employed to mitigate the effects of class imbalance
230 and to allow for a more accurate assessment of the model's performance in link
231 prediction.

232

233 We employed a VGA to compress the data and retrieve the latent features. The VGA
234 was evaluated on a complete version of the graph without removing any edges. To train
235 the model, we used the Adam optimization algorithm with an initial learning rate set to
236 a predefined value. The batch size was fixed at 1024, and we trained the model for a

237 total of 100 epochs. To mitigate the risk of overfitting, we applied L2 regularization
238 (weight decay) with a specified weight value. The learning rate adjustment function
239 used was the cosine annealing function, and the loss function employed was the cross-
240 entropy loss function. During training, we calculated the loss between the predicted
241 values and the ground truth. The model's parameters were then optimized by the Adam
242 optimization algorithm based on the calculated loss. To address the data imbalance
243 problem, we used a cost matrix to give more attention to false positives and omissions.

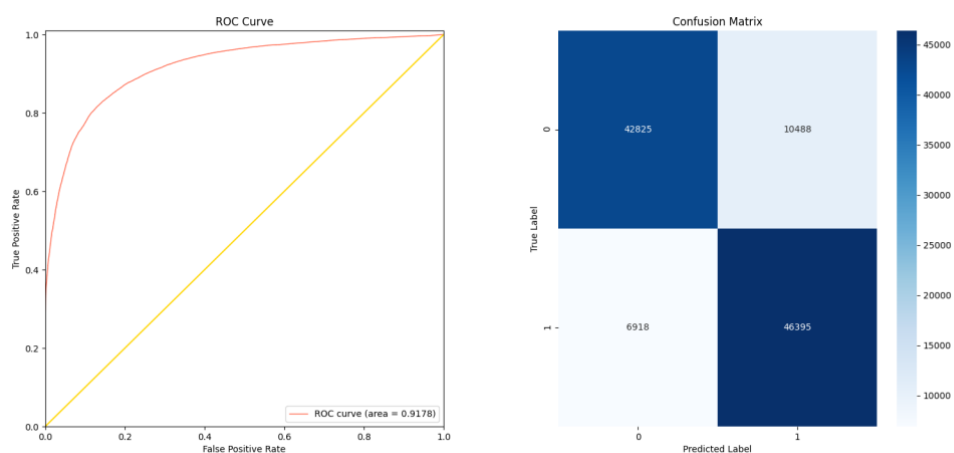


245 **Fig. 1. Overview of the graph-embedding convolution network (GECN)**
246 **algorithm.** The GECN algorithm combines graph embedding and graph
247 convolution network. A variational graph autoencoder learned embedding
248 gene features and protein interaction networks to latent features. DeepGCN
249 predicts disease-associated genes based on latent features.
250

251 3.2 Performance of the graph embedding convolution network algorithm

252 The performance of our deep learning model was evaluated using various metrics,
253 including the area under the receiver operating characteristic curve (AUC) and fixed-
254 threshold metrics such as accuracy, recall, precision, F1 score, and F2 score. The test
255 set achieved an AUC of 0.92 (Fig. 2a), while the accuracy of the model with the
256 threshold applied was 0.84, with a recall of 0.87 and a precision of 0.82 (Fig. 2b). The
257 F1 and F2 scores were 0.84 and 0.86, respectively. The confusion matrix of the test set
258 revealed 10,488 new predicted links, suggesting potential interactions between pairs of
259 genes that were not constrained to physical binding due to the nature of the STRING
260 dataset and may include metabolic pathways or cellular processes.

261



262

263 **Fig. 2. Evaluation of link prediction of the protein interaction network.**

264 The receiver operating characteristic (ROC) curve (a) and confusion matrix

265 (b) of link prediction were evaluated from the test set.

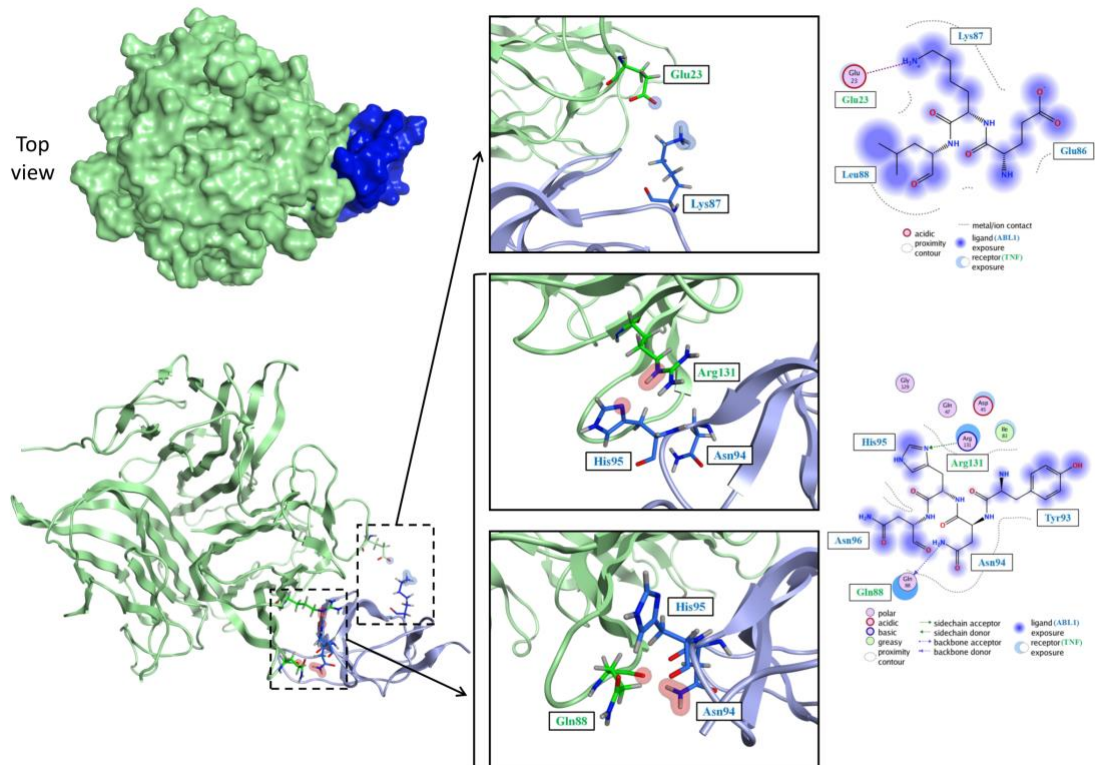
266

267 **3.3 Predicting and Assessing Protein-Protein Interactions between COVID-19** 268 **and Associated Genes through Molecular Docking Analysis**

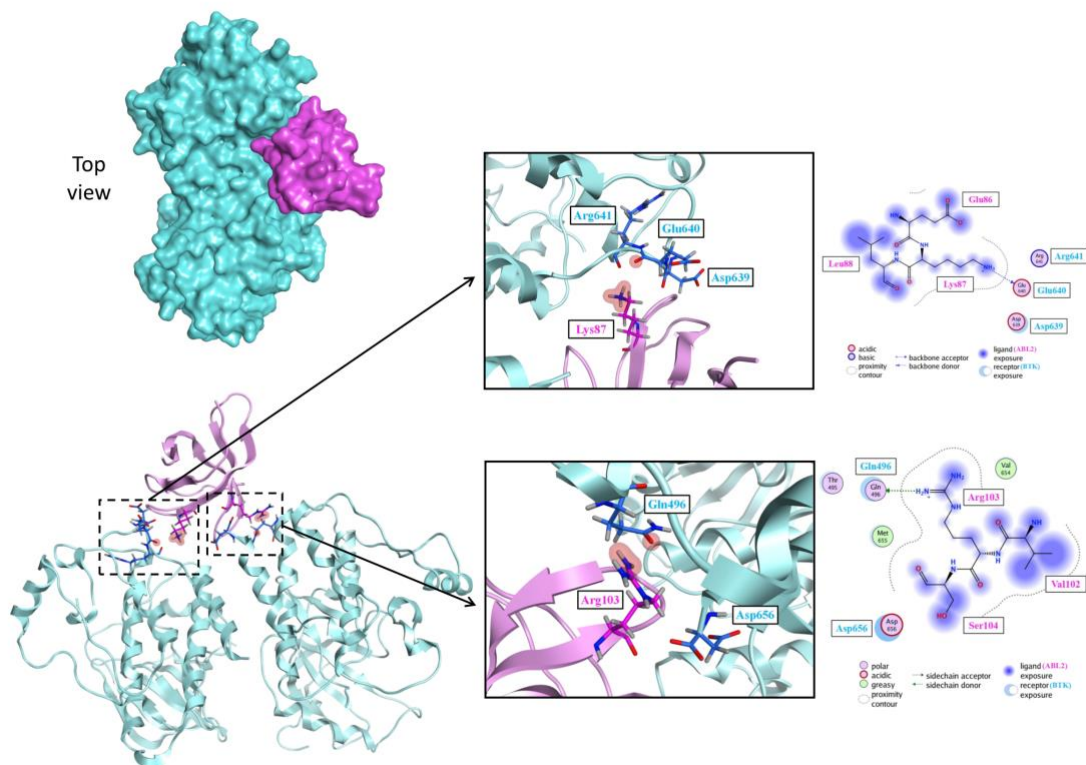
269 To understand virus-host protein interactions have found that SARS-CoV-2
270 can interfere with various signaling pathways in host cells. The immune evasion of
271 SARS-CoV-2 improves viral survival and triggers pathogenic mechanisms in host
272 cells. Analyzing the host protein associated with the known COVID-19 related
273 genes can reveal new druggable targets and can help heal COVID-19 patients by
274 blocking pathogenic signaling pathways or potential virus-host protein interactions.
275 Our analysis identified several predicted interacting genes that showed potential
276 associations with COVID-19-related genes ABL1 (39.13%) and ABL2 (26.09%).
277 Less than 1% of genes interacted with other COVID-19-related genes (see
278 Supplementary Table 1). Notably, ABL1-TNF and ABL2-BTK had the highest
279 probabilities of predicted links for ABL1 and ABL2, respectively.

280 To estimate the likelihood of physical binding in the predicted association, we
281 used the Molecular Operating Environment (MOE) software [34, 35]. We selected the
282 links with the highest probabilities of prediction and the docking structures of ABL1-
283 TNF and ABL2-BTK as candidates. Our analysis revealed that the best docking
284 structure of ABL1-TNF achieved an S score of -67.63 and a root-mean-square deviation
285 (RMSD) of 0.98, while ABL2-BTK achieved an S score of -51.39 and RMSD of 1.16,
286 indicating a high probability of physical interaction between these two pairs.

287 The 2D interaction diagram (Fig. 3) shows the three phenomena. First, amino acid
288 residues are exposed in solution. Second, binding pockets are formed. Finally, the
289 important amino acid residues are involved in protein interactions. For example, the
290 side chain of Arg131 on TNF forms a hydrogen bond with the side chain of His95 on
291 ABL1 (bond length = 3.345 Å, energy = 4.500 kcal/mol), the backbone of Gln88 on
292 TNF forms a hydrogen bond with the side chain of Asn94 on ABL1 (bond length =
293 3.205 Å, energy = 3.100 kcal/mol), and the side chain of Glu23 on TNF forms an ionic
294 bond with the side chain of Lys87 on ABL1 (bond length = 4.006 Å, energy = 0.501
295 kcal/mol). The backbone of Glu640 on BTK forms a hydrogen bond with the side chain
296 of Lys87 on ABL2 (bond length = 3.439 Å, bond energy = 1.300 kcal/mol), and the
297 side chain of Gln496 on BTK forms a hydrogen bond with the side chain of Arg103 on
298 ABL2 (bond length = 3.199 Å, bond energy = 0.700 kcal/mol).



299



300

301

302

303

Fig. 3. Docking structure with the lowest energy simulated by Molecular Operating Environment. The docking positions of the two proteins are clearly shown in Fig. 3 in the protein surface diagram (upper

304 left panel) and ribbon diagram (upper right panel). **(a)** Docking structures
305 of ABL1- tumor necrosis factor (TNF) and ABL1 (Protein Data Bank
306 (PDB) ID: 1AWO) are shown as blue ribbons, whereas those of TNF (PDB
307 ID: 1TNF) are shown as green ribbons; the skeletons are binding sites. **(b)**
308 Docking structures of ABL2- Bruton's tyrosine kinase (BTK) and ABL2
309 (PDB ID: 5NP3) are shown as pink ribbons and those of BTK (PDB ID:
310 5XYZ) are shown as green ribbons; the skeletons are binding sites.

311

312 **3.4 Predicting Potential Target Genes in SARS-CoV-2 Affected Host Protein** 313 **Networks using GECN Algorithm**

314 The GECN algorithm was tested using 15 COVID-19 associated genes from CTD
315 in 2019 as a graph center to construct SARS-CoV-2 affected host protein networks. The
316 algorithm embedded the latency features from the autoencoder, with an accuracy of
317 0.99 ± 0.01 (mean \pm SD), precision of 0.64 ± 0.11 , recall of 0.77 ± 0.15 , and F1 of 0.69
318 ± 0.08 . The top five predicted targets were Interleukin (IL)-4, Colony-stimulating factor
319 2 (CSF2), IL-13, CXCL8, and PRL; CXCL8 was confirmed as a COVID-19 associated
320 gene in 2021.

321 In the second stage, COVID-19 associated genes from CTD in 2021 were used as
322 the graph center to construct a SARS-CoV-2 affected host protein network. The
323 algorithm embedded the latency features from the autoencoder, with an accuracy of
324 0.99 ± 0.01 (mean \pm SD), precision of 0.69 ± 0.06 , recall of 0.80 ± 0.10 , and F1 of 0.74
325 ± 0.06 . The top three predicted targets were CSF2, IL-4, and IL-13. These target genes
326 include ALB1/ALB2 (which might be involved in the entry of SARS-CoV-2 into host
327 cells), CSF2 (which might participate in the cytokine storm, inducing severe
328 syndrome), and IL-4 and IL-13 (which might participate in pulmonary fibrosis).

329

330 **4. Discussion**

331 The efficacy and safety of the COVID-19 pandemic has resulted in significant
332 societal challenges. However, clinicians have no drug recommendations without a
333 proper understanding of the virus and its mechanisms. In this context, in silico
334 approaches led to the advancement of machine learning techniques and docking
335 methods in drug repurposing. In this study, we developed a deep learning algorithm,
336 the GECN, to predict COVID-19 related genes integrated with functional annotations
337 of human genes. However, focusing on specific targets such as spike protein, 3CL
338 protease, and MPro in SARS-CoV-2 or ACE2 and TMPRSS2 would restrict the
339 candidate screening scope. Most interactive proteins in humans are associated with
340 endomembrane compartments or vesicle trafficking pathways, indicating the essential
341 role of human proteins during infection. Therefore, this study identified 332 physical
342 interactions which provide form COVID-19 Research Group of Quantitative
343 Biosciences Institute between human proteins and SARS-CoV-2 proteins, providing a
344 comprehensive view of the host-pathogen interactome.

345 Our GECN algorithm predicted ABL1, ABL2, CSF2, IL-4, and IL-13 as
346 candidates for COVID-19 treatment target genes, which were successfully identified as
347 having a binding affinity with COVID-19-related proteins. The use of deep learning
348 algorithms, such as the GECN used in this study, can be a powerful tool for analyzing
349 large amounts of data and identifying patterns that may not be apparent to humans.
350 Previous studies [36, 37] on the ABL family and coronavirus the ABL kinase inhibitor,
351 GNF2, GNF5 [36], imatinib [36, 37], imatinib mesylate [38], nilotinib [38], and
352 dasatinib [38] can reduce the viral titer of coronavirus by preventing syncytia formation.
353 These results also suggest that ABL1 and ABL2 are involved in the process of
354 coronavirus infection. Experiments on ABL kinase inhibitor treatment of SARS-CoV-
355 2 have shown promising results that imatinib mesylate suppresses the replication of
356 SARS-CoV-2 in Vero-E6 cell[39]. Moreover, study on nilotinib, dasatinib, and
357 imatinib reported antiviral activity only of nilotinib but not of dasatinib or imatinib in
358 Vero-E6 cells and Calu-3 cells [40]. Imatinib did not exhibit any antiviral activity in
359 Caco-2 cells, as documented in a previous study [41]. Three randomized clinical trials
360 are currently underway to study imatinib's efficacy in treating COVID-19.
361 NCT04357613 (France), NCT04394416 (USA), and EudraCT2020-001236-10 (The
362 Netherlands), are currently underway to study the therapeutic efficacy of imatinib in
363 COVID-19 patients, controversial results are derived from different ABL kinase

364 inhibitors, and more studies are needed to determine its therapeutic effect. Furthermore,
365 the GECN-predicted targets, CSF2, IL-4, and IL-13, have been associated with
366 COVID-19 in previous clinical studies [42-44]. GM-CSF is involved in the
367 inflammatory phase, which induces a cytokine storm, and IL-4 and IL-13 are involved
368 in the tissue repair phase, which causes pulmonary fibrosis. Therefore, clinical trials
369 have focused on these three targets. Lenzilumab is a monoclonal antibody against GM-
370 CSF with high binding affinity and low immunogenicity [45]. Lenzilumab neutralizes
371 the GM-CSF effect and blocks signal transduction to myeloid progenitor cells.
372 Lenzilumab has been shown to reduce the risk of death or respiratory failure in
373 hospitalized COVID-19 patients [45]. Dupilumab is an IL-4R α antagonist used in the
374 treatment of atopic dermatitis, which blocks IL-13 and IL-4 signaling, may have
375 potential as a treatment for COVID-19. A retrospective analysis of a trial of two-cohorts
376 of patients infected with SARS-CoV2- confirmed the benefit with a lower risk of death
377 in patients.

378 In addition, recent studies have developed innovative models for designing picomolar
379 miniprotein inhibitors [4]. These models leverage computer-generated scaffolds
380 designed to optimize target binding, folding, and stability around an ACE2 helix that
381 interacts with the spike receptor binding domain or are docked against the RBD to
382 identify new binding modes. These de novo design approaches offer a innovative and
383 promising solution to the COVID crisis. However, clinicians have the critical timing of
384 the pandemic outbreak, there is a dire need for potent therapeutics immediatly.
385 Although designing drugs specific to SARS-CoV-2 is the gold standard solution, it
386 requires complex and time-consuming procedures. Our GECN algorithm is built up
387 with a knowledge database to further extend drug repurposing by summarizing
388 information on FDA-approved drugs that could be applied immediately.

389

390 **5. Conclusions**

391 This study highlights the potential of using deep learning algorithms to discover
392 potential therapeutic targets for COVID-19. Although our results were consistent with
393 those of several studies, our predictions were difficult to confirm without more
394 knowledge of virus-host interactions. The GECN identified several genes that may be
395 targets for COVID-19 treatment, including ABL1, ABL2, CSF2, IL-4, and IL-13.
396 Clinical trials have shown promising results for Lenzilumab, a monoclonal antibody
397 against GM-CSF. However, more studies are needed to confirm the effectiveness of

398 these drugs and their potential side effects. These findings provide a starting point for
399 further research into potential treatments for COVID-19.
400
401

402 **Key Points**

403 The graph-embedding convolution network (GECN), a novel deep learning
404 model, was developed to identify COVID-19-related genes and druggable
405 targets by analyzing COVID-19-related human protein interaction networks.

406 GECN identified several target genes, including ALB1/ALB2, CSF2, IL-4, and
407 IL-13, that are meaningfully correlated with COVID-19, potentially involved in
408 the entry of SARS-CoV-2 into host cells, cytokine storm, and pulmonary
409 fibrosis.

410 The GECN algorithm can predict COVID-19 drug targets rapidly, accurately,
411 and explainably, demonstrating its potential to expand our knowledge of disease
412 pathologies and accelerate drug discovery at a low cost.

413 **Declarations**

414

415 **Ethics approval and consent to participate**

416 All authors had ethical approval and consent to participate.

417

418 **Consent for publication**

419 All authors agreed with consent for publication.

420

421 **Availability of data and materials**

422

423 The data that support the findings of this study are available from the corresponding
424 author and listing authors upon reasonable request.

425

426 **Conflict of Interest**

427

428 All authors declare that they have no conflicts of interest.

429 **Funding**

430 This work was supported by the Ministry of Science and Technology [Grant numbers
431 MOST 110-2314-B-A49A-504-MY3, MOST 110-2926-I-010-504, MOST 108-2923-
432 B-010-002-MY3, MOST 109-2823-8-010-003-CV, MOST 109-2622-B-010-006,
433 MOST 110-2321-B-A49A-502, and MOST 110-2923-B-A49A-501-MY3]; the
434 Development and Construction Plan of the School of Medicine, National Yang-Ming
435 University, now known as National Yang Ming Chiao Tung University [Grant number

436 107F-M01-0504]; Aiming for the Top University Plan, a grant from the Ministry of
437 Education [Grant number MOST 109-2823-8-010-003-CV].

438 **Author contributions**

439 **Y-H.T.** conceptualized the study and wrote the methodology, original draft, and
440 funding acquisition. **H.H.** wrote the original draft and reviewed and edited the
441 manuscript. **C-N.Y.** contributed to the investigation, validation, formal analysis, and
442 methodology. **S-H.W.** contributed to study investigation, validation, manuscript
443 writing, review, and editing, and arranged resources. **O.K-S.L.** supervised the study,
444 managed the project, and contributed to manuscript writing, review, and editing.

445 **Acknowledgements**

446 The authors acknowledge financial support from the Ministry of Science and
447 Technology. The Development and Construction Plan of the School of Medicine,
448 National Yang-Ming University, now known as National Yang Ming Chiao Tung
449 University, and Aiming for the Top University Plan, a grant from the Ministry of
450 Education. We thank Muen Biomedical and Optoelectronics Technologies Inc. and all
451 our colleagues at National Yang Ming Chiao Tung University for their encouragement
452 and support.

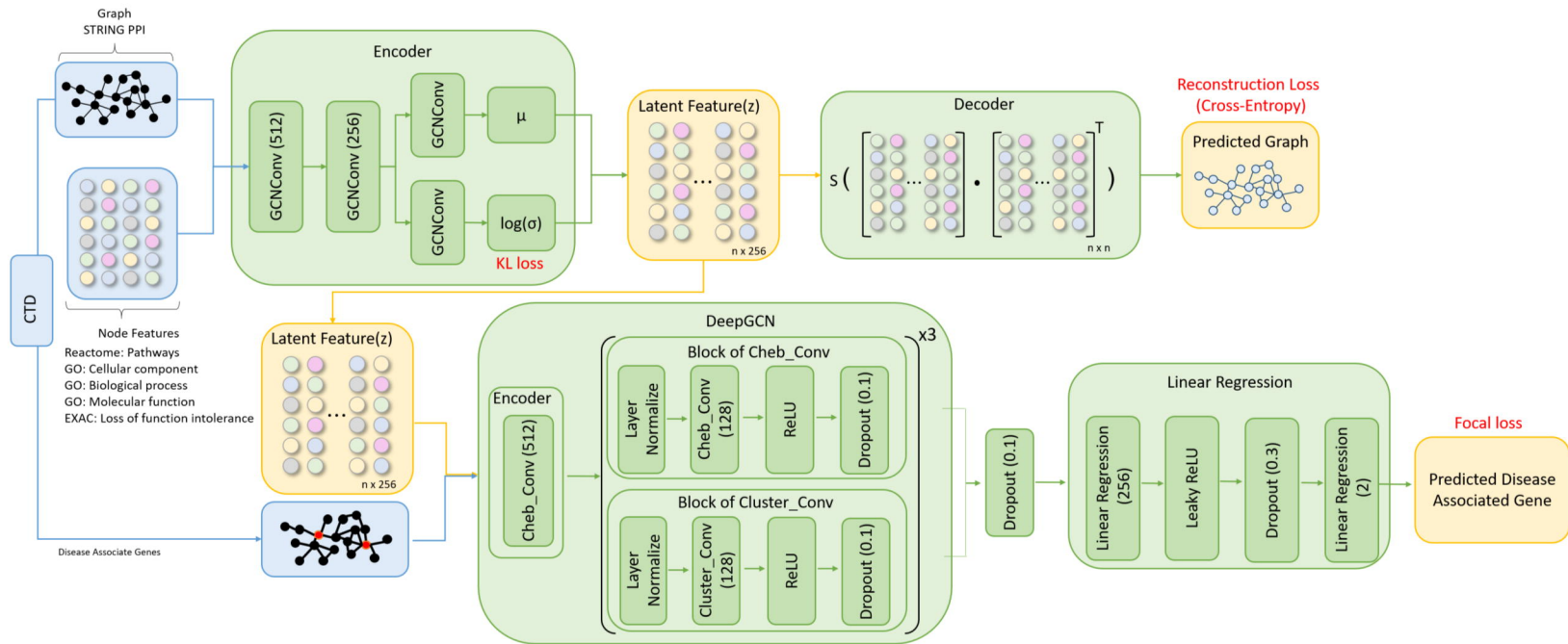
453

454 References

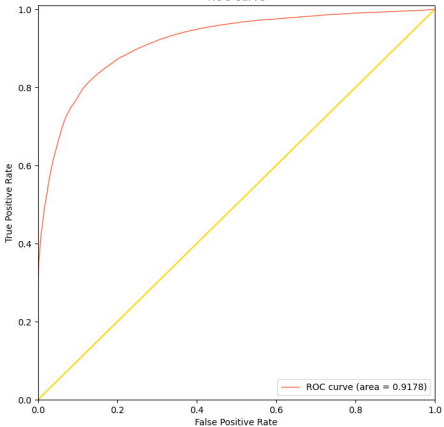
- 455 1. Chen N, Zhou M, Dong X, Qu J, Gong F, Han Y, Qiu Y, Wang J, Liu Y, Wei Y *et al*:
456 **Epidemiological and clinical characteristics of 99 cases of 2019 novel**
457 **coronavirus pneumonia in Wuhan, China: a descriptive study.** *Lancet* 2020,
458 **395(10223):507-513.**
- 459 2. Ragab D, Salah Eldin H, Taeimah M, Khattab R, Salem R: **The COVID-19**
460 **Cytokine Storm; What We Know So Far.** *Front Immunol* 2020, **11**:1446.
- 461 3. Singh TU, Parida S, Lingaraju MC, Kesavan M, Kumar D, Singh RK: **Drug**
462 **repurposing approach to fight COVID-19.** *Pharmacol Rep* 2020, **72(6):1479-**
463 **1508.**
- 464 4. Cao L, Goureshnik I, Coventry B, Case JB, Miller L, Kozodoy L, Chen RE, Carter L,
465 Walls AC, Park YJ *et al*: **De novo design of picomolar SARS-CoV-2 miniprotein**
466 **inhibitors.** *Science* 2020, **370(6515):426-431.**
- 467 5. Dauparas J, Anishchenko I, Bennett N, Bai H, Ragotte RJ, Milles LF, Wicky BIM,
468 Courbet A, de Haas RJ, Bethel N *et al*: **Robust deep learning-based protein**
469 **sequence design using ProteinMPNN.** *Science* 2022, **378(6615):49-56.**
- 470 6. Scarselli F, Gori M, Tsoi AC, Hagenbuchner M, Monfardini G: **The graph neural**
471 **network model.** *IEEE transactions on neural networks* 2008, **20(1):61-80.**
- 472 7. Zhang XM, Liang L, Liu L, Tang MJ: **Graph Neural Networks and Their Current**
473 **Applications in Bioinformatics.** *Front Genet* 2021, **12**:690049.
- 474 8. Bruna J, Zaremba W, Szlam A, LeCun Y: **Spectral networks and locally**
475 **connected networks on graphs.** *arXiv preprint arXiv:13126203* 2013.
- 476 9. Kipf TN, Welling M: **Semi-supervised classification with graph convolutional**
477 **networks.** *arXiv preprint arXiv:160902907* 2016.
- 478 10. Veličković P, Cucurull G, Casanova A, Romero A, Lio P, Bengio Y: **Graph**
479 **attention networks.** *arXiv preprint arXiv:171010903* 2017.
- 480 11. Yin W, Mao C, Luan X, Shen DD, Shen Q, Su H, Wang X, Zhou F, Zhao W, Gao M
481 *et al*: **Structural basis for inhibition of the RNA-dependent RNA polymerase**
482 **from SARS-CoV-2 by remdesivir.** *Science* 2020, **368(6498):1499-1504.**
- 483 12. Beigel JH, Tomashek KM, Dodd LE, Mehta AK, Zingman BS, Kalil AC, Hohmann
484 E, Chu HY, Luetkemeyer A, Kline S *et al*: **Remdesivir for the Treatment of Covid-**
485 **19 - Final Report.** *N Engl J Med* 2020, **383(19):1813-1826.**
- 486 13. Ge Y, Tian T, Huang S, Wan F, Li J, Li S, Wang X, Yang H, Hong L, Wu N *et al*: **An**
487 **integrative drug repositioning framework discovered a potential therapeutic**
488 **agent targeting COVID-19.** *Signal Transduct Target Ther* 2021, **6(1):165.**
- 489 14. Martin WR, Cheng F: **Repurposing of FDA-Approved Toremifene to Treat**
490 **COVID-19 by Blocking the Spike Glycoprotein and NSP14 of SARS-CoV-2.** *J*
491 *Proteome Res* 2020, **19(11):4670-4677.**
- 492 15. Zeng X, Song X, Ma T, Pan X, Zhou Y, Hou Y, Zhang Z, Li K, Karypis G, Cheng F:
493 **Repurpose open data to discover therapeutics for COVID-19 using deep**
494 **learning.** *Journal of proteome research* 2020, **19(11):4624-4636.**
- 495 16. Richardson P, Griffin I, Tucker C, Smith D, Oechsle O, Phelan A, Rawling M,
496 Savory E, Stebbing J: **Baricitinib as potential treatment for 2019-nCoV acute**
497 **respiratory disease.** *Lancet* 2020, **395(10223):e30-e31.**
- 498 17. Zhou Y, Hou Y, Shen J, Kallianpur A, Zein J, Culver DA, Farha S, Comhair S,
499 Fiocchi C, Gack MU *et al*: **A Network Medicine Approach to Investigation and**
500 **Population-based Validation of Disease Manifestations and Drug**

- 501 **Repurposing for COVID-19.** *ChemRxiv* 2020.
- 502 18. Horby P, Lim WS, Emberson JR, Mafham M, Bell JL, Linsell L, Staplin N,
503 Brightling C, Ustianowski A, Elmahi E *et al*: **Dexamethasone in Hospitalized**
504 **Patients with Covid-19.** *N Engl J Med* 2021, **384**(8):693-704.
- 505 19. Fadaka AO, Sibuyi NRS, Madiehe AM, Meyer M: **Computational insight of**
506 **dexamethasone against potential targets of SARS-CoV-2.** *J Biomol Struct Dyn*
507 2022, **40**(2):875-885.
- 508 20. Goldman JD, Lye DCB, Hui DS, Marks KM, Bruno R, Montejano R, Spinner CD,
509 Galli M, Ahn MY, Nahass RG *et al*: **Remdesivir for 5 or 10 Days in Patients with**
510 **Severe Covid-19.** *N Engl J Med* 2020, **383**(19):1827-1837.
- 511 21. Szkarczyk D, Gable AL, Lyon D, Junge A, Wyder S, Huerta-Cepas J, Simonovic
512 M, Doncheva NT, Morris JH, Bork P *et al*: **STRING v11: protein-protein**
513 **association networks with increased coverage, supporting functional**
514 **discovery in genome-wide experimental datasets.** *Nucleic Acids Res* 2019,
515 **47**(D1):D607-d613.
- 516 22. Ashburner M, Ball CA, Blake JA, Botstein D, Butler H, Cherry JM, Davis AP,
517 Dolinski K, Dwight SS, Eppig JT *et al*: **Gene ontology: tool for the unification of**
518 **biology. The Gene Ontology Consortium.** *Nat Genet* 2000, **25**(1):25-29.
- 519 23. Fabregat A, Sidiropoulos K, Viteri G, Marin-Garcia P, Ping P, Stein L, D'Eustachio
520 P, Hermjakob H: **Reactome diagram viewer: data structures and strategies to**
521 **boost performance.** *Bioinformatics* 2018, **34**(7):1208-1214.
- 522 24. Alanazi A, Nojiri C, Noguchi T, Kido T, Komatsu Y, Hirakuri K, Funakubo A, Sakai
523 K, Fukui Y: **Improved Blood Compatibility of DLC Coated Polymeric Material.**
524 *ASAIO Journal* 2000, **46**(4):440-443.
- 525 25. **UniProt: a worldwide hub of protein knowledge.** *Nucleic Acids Res* 2019,
526 **47**(D1):D506-d515.
- 527 26. Jassal B, Matthews L, Viteri G, Gong C, Lorente P, Fabregat A, Sidiropoulos K,
528 Cook J, Gillespie M, Haw R *et al*: **The reactome pathway knowledgebase.**
529 *Nucleic Acids Res* 2020, **48**(D1):D498-d503.
- 530 27. Lek M, Karczewski KJ, Minikel EV, Samocha KE, Banks E, Fennell T, O'Donnell-
531 Luria AH, Ware JS, Hill AJ, Cummings BB *et al*: **Analysis of protein-coding**
532 **genetic variation in 60,706 humans.** *Nature* 2016, **536**(7616):285-291.
- 533 28. Davis AP, Grondin CJ, Johnson RJ, Sciaky D, Wiegiers J, Wiegiers TC, Mattingly
534 CJ: **Comparative Toxicogenomics Database (CTD): update 2021.** *Nucleic Acids*
535 *Research* 2020, **49**(D1):D1138-D1143.
- 536 29. Anno S, Hirakawa T, Sugita S, Yasumoto S: **A graph convolutional network for**
537 **predicting COVID-19 dynamics in 190 regions/countries.** *Front Public Health*
538 2022, **10**:911336.
- 539 30. Kingma DP, Ba J: **Adam: A method for stochastic optimization.** *arXiv preprint*
540 *arXiv:1412.6980* 2014.
- 541 31. Wu Z, Pan S, Chen F, Long G, Zhang C, Philip SY: **A comprehensive survey on**
542 **graph neural networks.** *IEEE transactions on neural networks and learning*
543 *systems* 2020, **32**(1):4-24.
- 544 32. Chiang W-L, Liu X, Si S, Li Y, Bengio S, Hsieh C-J: **Cluster-gcn: An efficient**
545 **algorithm for training deep and large graph convolutional networks.** In:
546 *Proceedings of the 25th ACM SIGKDD international conference on knowledge*
547 *discovery & data mining: 2019.* 257-266.

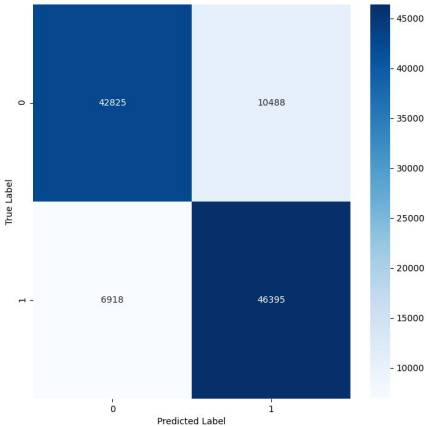
- 548 33. Inc. CCG: **Molecular operating environment (MOE)**. In.: Chemical Computing
549 Group Inc. Montreal, QC, Canada; 2016.
- 550 34. Aleman MM, Walton BL, Byrnes JR, Wolberg AS: **Fibrinogen and red blood cells**
551 **in venous thrombosis**. *Thromb Res* 2014, **133 Suppl 1**(0 1):S38-40.
- 552 35. Clark AM, Labute P: **2D depiction of protein– ligand complexes**. *Journal of*
553 *chemical information and modeling* 2007, **47**(5):1933-1944.
- 554 36. Sisk JM, Frieman MB, Machamer CE: **Coronavirus S protein-induced fusion is**
555 **blocked prior to hemifusion by Abl kinase inhibitors**. *The Journal of general*
556 *virology* 2018, **99**(5):619.
- 557 37. Coleman CM, Sisk JM, Mingo RM, Nelson EA, White JM, Frieman MB: **Abelson**
558 **kinase inhibitors are potent inhibitors of severe acute respiratory syndrome**
559 **coronavirus and Middle East respiratory syndrome coronavirus fusion**.
560 *Journal of virology* 2016, **90**(19):8924-8933.
- 561 38. Dyall J, Coleman CM, Venkataraman T, Holbrook MR, Kindrachuk J, Johnson RF,
562 Olinger Jr GG, Jahrling PB, Laidlaw M, Johansen LM: **Repurposing of clinically**
563 **developed drugs for treatment of Middle East respiratory syndrome**
564 **coronavirus infection**. *Antimicrobial agents and chemotherapy* 2014,
565 **58**(8):4885-4893.
- 566 39. Sauvat A, Ciccocanti F, Colavita F, Di Rienzo M, Castilletti C, Capobianchi MR,
567 Kepp O, Zitvogel L, Fimia GM, Piacentini M: **On-target versus off-target effects**
568 **of drugs inhibiting the replication of SARS-CoV-2**. *Cell Death & Disease* 2020,
569 **11**(8):656.
- 570 40. Cagno V, Magliocco G, Tapparel C, Daali Y: **The tyrosine kinase inhibitor**
571 **nilotinib inhibits SARS-CoV-2 in vitro**. *Basic & clinical pharmacology &*
572 *toxicology* 2021, **128**(4):621-624.
- 573 41. Zhao H, Mendenhall M, Deininger MW: **Imatinib is not a potent anti-SARS-**
574 **CoV-2 drug**. *Leukemia* 2020, **34**(11):3085-3087.
- 575 42. Thwaites R: **Sanchez Sevilla Uruchurtu A, Siggins MK, et al. Inflammatory**
576 **profiles across the spectrum of disease reveal a distinct role for GM-CSF in**
577 **severe COVID-19** *Sci Immunol* 2021, **6**(57):57.
- 578 43. Donlan AN, Sutherland TE, Marie C, Preissner S, Bradley BT, Carpenter RM,
579 Sturek JM, Ma JZ, Moreau GB, Donowitz JR: **IL-13 is a driver of COVID-19**
580 **severity**. *JCI insight* 2021, **6**(15).
- 581 44. Shenoy S: **SARS-CoV-2 (COVID-19), viral load and clinical outcomes; lessons**
582 **learned one year into the pandemic: a systematic review**. *World Journal of*
583 *Critical Care Medicine* 2021, **10**(4):132.
- 584 45. Temesgen Z, Assi M, Shweta F, Vergidis P, Rizza SA, Bauer PR, Pickering BW,
585 Razonable RR, Libertin CR, Burger CD: **GM-CSF neutralization with lenzilumab**
586 **in severe COVID-19 pneumonia: a case-cohort study**. In: *Mayo Clinic*
587 *Proceedings: 2020*. Elsevier: 2382-2394.
- 588



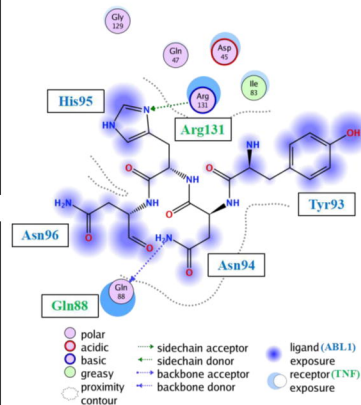
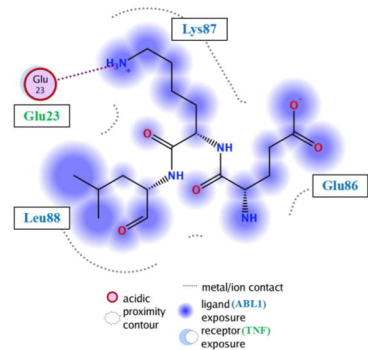
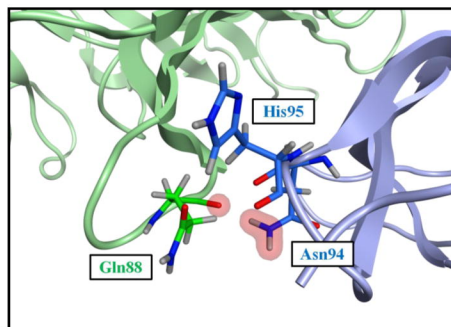
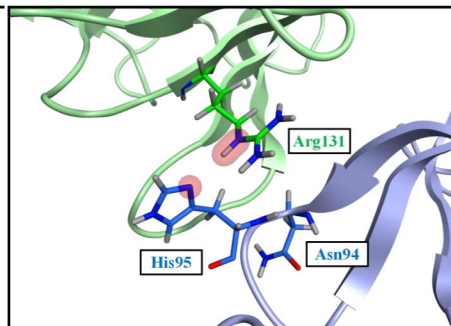
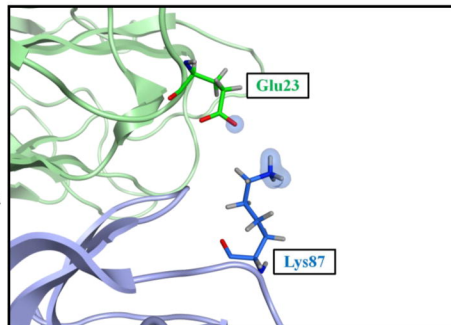
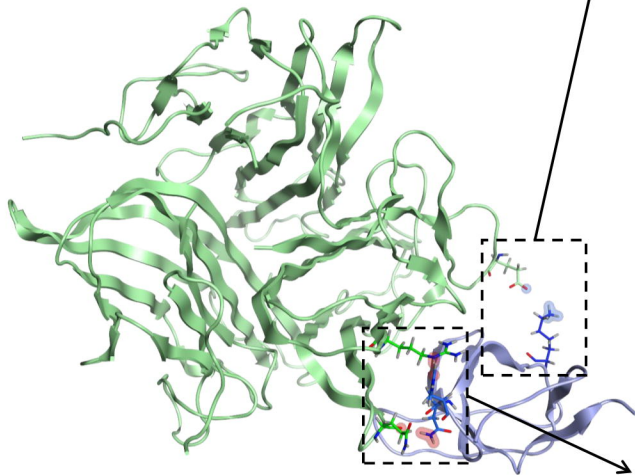
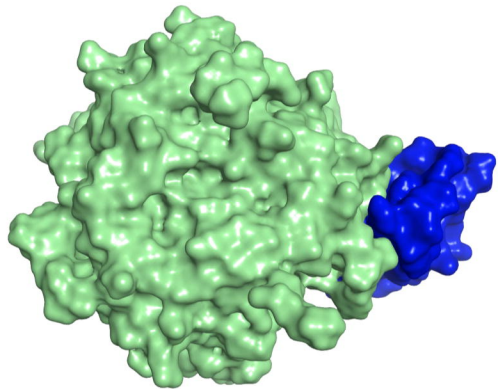
ROC Curve



Confusion Matrix



Top view



Top view

